



**INTEGRATED GPR AND LASER VIBRATION SURVEYS TO  
PRESERVE PREHISTORICAL PAINTED CAVES: CUEVA  
PINTADA CASE STUDY**

Journal:	<i>International Journal of Architectural Heritage</i>
Manuscript ID	UARC-2019-2492.R1
Manuscript Type:	Original Article
Date Submitted by the Author:	n/a
Complete List of Authors:	Caselles, Oriol; Universitat Politècnica de Catalunya, Ingeniería del Terreno, Cartografía y Geofísica Clapés, Jaume; Universitat Politècnica de Catalunya, Ingeniería del Terreno, Cartografía y Geofísica Rodríguez-Santana, Jose-Ignacio; Museo y Parque Arqueológico Cueva Pintada (Cabildo de Gran Canaria) Perez-Gracia, Vega; Universitat Politècnica de Catalunya, Resistencia de Materiales y Estructuras en la Ingeniería Rodríguez-Santana, Carmen-Gloria; Museo y Parque Arqueológico Cueva Pintada (Cabildo de Gran Canaria)
Keywords:	GPR, Laser Vibration, Painted Cave, Cueva Pintada, Amplification, Detachment

SCHOLARONE™  
Manuscripts

1  
2  
3 INTEGRATED GPR AND LASER VIBRATION SURVEYS TO PRESERVE  
4  
5 PREHISTORICAL PAINTED CAVES: CUEVA PINTADA CASE STUDY  
6  
7  
8  
9  
10

11 J.O. Caselles<sup>a</sup>, J. Clapés<sup>1a</sup>, J.I. Sáenz Sagasti<sup>b</sup>, V. Pérez Gracia<sup>c</sup> and C.G. Rodríguez Santana<sup>d</sup>  
12  
13

14 <sup>a</sup> DECA. Universitat Politècnica de Catalunya. c/ Jordi Girona 1. 08034 Barcelona. Spain  
15  
16

17 <sup>b</sup> Museo y Parque Arqueológico Cueva Pintada. Spain  
18  
19

20 <sup>c</sup> Department of Strength of Materials and Structural Engineering (RMEE), Polytechnic  
21 University of Catalonia (BarcelonaTech), Barcelona, Spain  
22  
23

24  
25 Correspondence : J.O. Caselles, DECA. Universitat Politècnica de Catalunya. c/ Jordi Girona  
26  
27

28 1. 08034 Barcelona. Spain. Email: oriol.caselles@upc.edu  
29  
30  
31  
32  
33  
34  
35  
36  
37  
38  
39  
40  
41  
42  
43  
44  
45  
46  
47  
48  
49  
50  
51  
52  
53  
54  
55  
56  
57  
58  
59  
60

## Abstract

The study of structural safety when it is covered by important paintings require a careful analysis without affecting the paintings. Therefore, non-destructive surveys are the only feasible method to obtain data about its state. In Cueva Pintada case, the problem requires a detailed but noninvasive analysis because this cave was dug in volcanic tuff. The tuff present poor consolidation. This geological material is very sensitive to vibration. Furthermore, the proximity to the city downtown increases vibrations due to traffic. Recently, a small rock fall produces damage and alerted of the cave state of conservation.

The painting walls constraint many of the NDT surveys. Two methodologies have been applied: ground-penetrating radar (GPR) and passive seismic. GPR analysis allowed determining the inner structure of the tuff cave, and results were used to determine the zones that required a wider and dense vibration study. Radar images shown important anomalies at depths of about 0.2 m to 0.8 meters and from 1.5 meters to the top of the roof, almost horizontal. Amplification factor measured by passive seismic survey range from 0.03 to 93 with near half of the ceil with amplifications higher than 5 and about 10% with amplifications over 50 times.

Keywords: GPR; Laser Vibration; Painted Cave; Cueva Pintada; Amplification, Detachment.

## Introduction

Cueva Pintada is part of a huge complex of artificial caves, located near Galdar, in Northwest Gran Canaria Island. This cave was excavated in volcanic tuff and belonged to a Pre-

1  
2  
3 Hispanic village. The most remarkable feature of this cave is the existence of geometrical  
4 wall paintings covering the walls (Fig. 1a). These paintings present triangles, rectangles,  
5 circles and squares, combining red, black and white colours. The archaeological space of the  
6  
7  
8 Cueva Pintada constitutes a key reference point in the study of the pre-Hispanic world of  
9  
10 Gran Canaria. The cave presents approximately a cubic 3 m height shape. The length of the  
11  
12  
13  
14  
15 back wall is 5 m, and the length of the lateral walls are 4.53 m and 4.26 m.

16  
17  
18 During the 19th century, the increase in construction and farming brought to find many  
19  
20  
21  
22  
23  
24  
25  
26  
27  
28  
29  
30  
31  
32  
33  
34  
35  
36  
37  
38  
39  
40  
41  
42  
43  
44  
45  
46  
47  
48  
49  
50  
51  
52  
53  
54  
55  
56  
57  
58  
59  
60  
61  
62  
63  
64  
65  
66  
67  
68  
69  
70  
71  
72  
73  
74  
75  
76  
77  
78  
79  
80  
81  
82  
83  
84  
85  
86  
87  
88  
89  
90  
91  
92  
93  
94  
95  
96  
97  
98  
99  
100  
101  
102  
103  
104  
105  
106  
107  
108  
109  
110  
111  
112  
113  
114  
115  
116  
117  
118  
119  
120  
121  
122  
123  
124  
125  
126  
127  
128  
129  
130  
131  
132  
133  
134  
135  
136  
137  
138  
139  
140  
141  
142  
143  
144  
145  
146  
147  
148  
149  
150  
151  
152  
153  
154  
155  
156  
157  
158  
159  
160  
161  
162  
163  
164  
165  
166  
167  
168  
169  
170  
171  
172  
173  
174  
175  
176  
177  
178  
179  
180  
181  
182  
183  
184  
185  
186  
187  
188  
189  
190  
191  
192  
193  
194  
195  
196  
197  
198  
199  
200  
201  
202  
203  
204  
205  
206  
207  
208  
209  
210  
211  
212  
213  
214  
215  
216  
217  
218  
219  
220  
221  
222  
223  
224  
225  
226  
227  
228  
229  
230  
231  
232  
233  
234  
235  
236  
237  
238  
239  
240  
241  
242  
243  
244  
245  
246  
247  
248  
249  
250  
251  
252  
253  
254  
255  
256  
257  
258  
259  
260  
261  
262  
263  
264  
265  
266  
267  
268  
269  
270  
271  
272  
273  
274  
275  
276  
277  
278  
279  
280  
281  
282  
283  
284  
285  
286  
287  
288  
289  
290  
291  
292  
293  
294  
295  
296  
297  
298  
299  
300  
301  
302  
303  
304  
305  
306  
307  
308  
309  
310  
311  
312  
313  
314  
315  
316  
317  
318  
319  
320  
321  
322  
323  
324  
325  
326  
327  
328  
329  
330  
331  
332  
333  
334  
335  
336  
337  
338  
339  
340  
341  
342  
343  
344  
345  
346  
347  
348  
349  
350  
351  
352  
353  
354  
355  
356  
357  
358  
359  
360  
361  
362  
363  
364  
365  
366  
367  
368  
369  
370  
371  
372  
373  
374  
375  
376  
377  
378  
379  
380  
381  
382  
383  
384  
385  
386  
387  
388  
389  
390  
391  
392  
393  
394  
395  
396  
397  
398  
399  
400  
401  
402  
403  
404  
405  
406  
407  
408  
409  
410  
411  
412  
413  
414  
415  
416  
417  
418  
419  
420  
421  
422  
423  
424  
425  
426  
427  
428  
429  
430  
431  
432  
433  
434  
435  
436  
437  
438  
439  
440  
441  
442  
443  
444  
445  
446  
447  
448  
449  
450  
451  
452  
453  
454  
455  
456  
457  
458  
459  
460  
461  
462  
463  
464  
465  
466  
467  
468  
469  
470  
471  
472  
473  
474  
475  
476  
477  
478  
479  
480  
481  
482  
483  
484  
485  
486  
487  
488  
489  
490  
491  
492  
493  
494  
495  
496  
497  
498  
499  
500  
501  
502  
503  
504  
505  
506  
507  
508  
509  
510  
511  
512  
513  
514  
515  
516  
517  
518  
519  
520  
521  
522  
523  
524  
525  
526  
527  
528  
529  
530  
531  
532  
533  
534  
535  
536  
537  
538  
539  
540  
541  
542  
543  
544  
545  
546  
547  
548  
549  
550  
551  
552  
553  
554  
555  
556  
557  
558  
559  
560  
561  
562  
563  
564  
565  
566  
567  
568  
569  
570  
571  
572  
573  
574  
575  
576  
577  
578  
579  
580  
581  
582  
583  
584  
585  
586  
587  
588  
589  
590  
591  
592  
593  
594  
595  
596  
597  
598  
599  
600  
601  
602  
603  
604  
605  
606  
607  
608  
609  
610  
611  
612  
613  
614  
615  
616  
617  
618  
619  
620  
621  
622  
623  
624  
625  
626  
627  
628  
629  
630  
631  
632  
633  
634  
635  
636  
637  
638  
639  
640  
641  
642  
643  
644  
645  
646  
647  
648  
649  
650  
651  
652  
653  
654  
655  
656  
657  
658  
659  
660  
661  
662  
663  
664  
665  
666  
667  
668  
669  
670  
671  
672  
673  
674  
675  
676  
677  
678  
679  
680  
681  
682  
683  
684  
685  
686  
687  
688  
689  
690  
691  
692  
693  
694  
695  
696  
697  
698  
699  
700  
701  
702  
703  
704  
705  
706  
707  
708  
709  
710  
711  
712  
713  
714  
715  
716  
717  
718  
719  
720  
721  
722  
723  
724  
725  
726  
727  
728  
729  
730  
731  
732  
733  
734  
735  
736  
737  
738  
739  
740  
741  
742  
743  
744  
745  
746  
747  
748  
749  
750  
751  
752  
753  
754  
755  
756  
757  
758  
759  
760  
761  
762  
763  
764  
765  
766  
767  
768  
769  
770  
771  
772  
773  
774  
775  
776  
777  
778  
779  
780  
781  
782  
783  
784  
785  
786  
787  
788  
789  
790  
791  
792  
793  
794  
795  
796  
797  
798  
799  
800  
801  
802  
803  
804  
805  
806  
807  
808  
809  
810  
811  
812  
813  
814  
815  
816  
817  
818  
819  
820  
821  
822  
823  
824  
825  
826  
827  
828  
829  
830  
831  
832  
833  
834  
835  
836  
837  
838  
839  
840  
841  
842  
843  
844  
845  
846  
847  
848  
849  
850  
851  
852  
853  
854  
855  
856  
857  
858  
859  
860  
861  
862  
863  
864  
865  
866  
867  
868  
869  
870  
871  
872  
873  
874  
875  
876  
877  
878  
879  
880  
881  
882  
883  
884  
885  
886  
887  
888  
889  
890  
891  
892  
893  
894  
895  
896  
897  
898  
899  
900  
901  
902  
903  
904  
905  
906  
907  
908  
909  
910  
911  
912  
913  
914  
915  
916  
917  
918  
919  
920  
921  
922  
923  
924  
925  
926  
927  
928  
929  
930  
931  
932  
933  
934  
935  
936  
937  
938  
939  
940  
941  
942  
943  
944  
945  
946  
947  
948  
949  
950  
951  
952  
953  
954  
955  
956  
957  
958  
959  
960  
961  
962  
963  
964  
965  
966  
967  
968  
969  
970  
971  
972  
973  
974  
975  
976  
977  
978  
979  
980  
981  
982  
983  
984  
985  
986  
987  
988  
989  
990  
991  
992  
993  
994  
995  
996  
997  
998  
999  
1000

During the 19th century, the increase in construction and farming brought to find many  
aboriginal remains and, being discovered Cueva Pintada as a result of the reform of an orchard  
in 1862. The archaeological works undertaken over more than two decades confirmed that the  
village was occupied from the 7th to the 16th centuries, being the last periods the best  
documented because archaeological discoveries are complemented with valuable written  
information (including travel writing, conquest chronicles and legal documents). Although, it  
is possible that the use of the cave and old constructions have been changed over time, we  
know that when the man-made cave was discovered, mummies, pottery and other  
archaeological objects were found. This fact suggests the space was probably designed for the  
celebration of offerings and ceremonies related to the dead.

In 1972, the set of caves were opened to the public after deep studies. Unfortunately, the  
deterioration of the paintings led to the closure of the Cueva Pintada in 1982, and the  
subsequent creation of a complete plan focused in the preservation of the pre-Hispanic  
legacy. As a result of this project, begun in 1986, the modern Museum and Archaeological  
Park Cueva Pintada (Fig. 1b) was inaugurated on the 26th July, 2006.

The pre-Hispanic ruins in this area were covered by the soil that was placed and distributed  
by the man in order to create farming terraces. Excavations indicate that the ruins belong to a  
hamlet organized around the group of man-made caves, known as the Troglodyte Complex.

1  
2  
3 The decorated chamber, known as Cueva Pintada, was in the center of the hamlet (Figure 1a).

4  
5 The agricultural landscape gradually disappeared as the excavations, begun in 1987,  
6 progressively brought to light the indigenous remains, and revealed a new archaeological  
7  
8 space.  
9

10  
11  
12  
13 The excavations during this long period have allowed discover and recover innumerable  
14 archaeological remains. These findings have been of great importance to understand the  
15 context of the aboriginal cultures of the Canary Islands. Other findings are probably imported  
16 from the continent. The discovered objects during the excavations include several ceramic  
17 pots elaborated in potter wheels and metal objects such as coins, swords, knives, horseshoes,  
18 thimbles, nails, etc. The current aspect of the Troglodyte complex, according to the available  
19 archaeological data, was most likely achieve after the 12th century, belonging the painted  
20 panel of the cave to this period.  
21  
22  
23  
24  
25  
26  
27  
28  
29  
30

31  
32 The study of the paintings indicates that the coloring agents are of mineral origin: oxidized  
33  
34 clays for ochre and red and, fine whitened clays for the white. Both were mixed with water to  
35 make their application easier. The black color was not a pigment but a natural darkening of  
36  
37 the tuff.  
38  
39  
40

41  
42 Currently, a triaxial accelerometer placed in one of the Troglodyte rooms, close to the painted  
43 cave constantly monitored Cueva Pintada (Soler at al., 2007). This supervising system was  
44 installed with the objective of monitoring the vibrations produced during the construction of  
45  
46 the new museum. Nowadays, this system alert of strong vibrations. However, at beginning of  
47  
48 2016, a slight sand detachment inside the cave occurred without any important recorded  
49  
50 vibration. That detachment forced to a wide study in order to determine possible causes and  
51  
52 to preserve the complex, preventing further detachments. Part of the study included a detailed  
53  
54  
55  
56  
57  
58  
59  
60

1  
2  
3 amplification vibration study. Before the vibration analysis, a high-resolution 3D GPR study  
4  
5 was used to calculate the best places to determine the amplification at each point of the cover.  
6  
7

8 Ground Penetrating Radar has been extensively used in a large number of archeological sites  
9  
10 (e.g., Zaho et al., 2013; Perez-Gracia et al. 2012; Perez-Gracia et al., 2009; Whiting et al.,  
11  
12 2001; Perez-Gracia et al., 2000) and cultural heritage structures (e.g., Perez-Gracia, 2013;  
13  
14 Cataldo, 2005; Ranalli et al., 2004). The archaeological studies were usually focused on  
15  
16 detecting and mapping buried structures (e.g., Nuzzo et al., 2002; Sternberg and McGill,  
17  
18 1995), on analyzing the extension of the archaeological site or even on evaluating  
19  
20 characteristics of the GPR received signal in order to correlate them with different  
21  
22 archaeological features (Zhao et al. 2015; Zhao et al. 2013). Archaeological applications are  
23  
24 based in many cases in 3D analysis by obtaining slices at different depths. The Cultural  
25  
26 Heritage assessment use to be centered in the detection of pathologies in the structures such  
27  
28 as moisture, cracks and detachments (e.g., Cataldo et al., 2005; Ferrara and Barone, 2015;  
29  
30 Santos-Assunção et al., 2014; Perez-Gracia et al., 2013; Solla et al., 2011). In some cases,  
31  
32 these studies are also applied to underground man-made structures (Santos-Assunção et al.,  
33  
34 2016) or to locate unknown constructive elements or other buried structures (Perez-Gracia et  
35  
36 al., 2009a; Perez-Gracia et al., 2009b; Gonzalez-Drigo et al., 2008). However, GPR studies  
37  
38 has been applied in few occasions in the study of rock caves and, in almost all the few cases,  
39  
40 mainly focused in detecting or mapping the cavities (e.g., Čeru et al., 2018; Zhao et al., 2012;  
41  
42 Beres et al., 2001) and in a minor number of cases, in the searching for buried archaeological  
43  
44 targets in caves (Porsani et al., 2010). The main difficult in the use of GPR inside caves leads  
45  
46 in two factors: the clutter and the irregular surface. Clutter is usually produced as  
47  
48 consequence of reflections on the walls and roofs close to the antenna, and obscures the  
49  
50 records because the external anomalies are superimposed to the anomalies produced by the  
51  
52  
53  
54  
55  
56  
57  
58  
59  
60

1  
2  
3 reflections on the subsurface features. The irregular surface habitual in many caves  
4  
5 complicates the radar data acquisition and introduces noise in the radargrams.  
6  
7

8  
9 Laser vibrometer has been used in art diagnostic applications (i.e. Castellini et al, 1996 and  
10  
11 2003; Borri and Grazini, 2006; Quagliarini et al., 2013). In all cases, the artworks  
12  
13 have been excited by some actuator or loudspeakers with white noise. The **ambient**  
14  
15 noise is similar to a white noise (Caselles et al., 2018). Laser vibrometer has been also  
16  
17 applied to civil engineering (p.e. Fukusda et al., 2010; Siringoringo and Fujino, 2009;  
18  
19 Waldron et al., 2002) and in mining engineering (p.e., Swanson, 2002). Frequencies  
20  
21 amplified in some loose roof rock in mines range from 200 to 1000 Hz (Summerfield,  
22  
23 1956; de Montille and Weber, 1971; Palmer and Czirr, 1982; Hanson, 1985). In  
24  
25 general, mines have a very hard rocks compared with the volcanic stuff of Galdar.  
26  
27 Pyroclastic materials can **present** shear velocities less than 200 m/s (Nunziata et al.,  
28  
29 1999).  
30  
31  
32  
33  
34  
35

36 Both geophysical surveys were used in the assessment of Cueva Pintada. GPR data and a  
37  
38 careful visual inspection determined the points to be surveyed using vibrations, based on  
39  
40 mapping the damage in the cave.  
41  
42  
43  
44  
45  
46

### 47 **Geological setting**

48  
49 Cueva Pintada is located less than 500 meters from the Galdar volcano. This volcano is of  
50  
51 Stromboli type, so pyroclastic materials compose the ground in an area of about 1.9 km<sup>2</sup>. In  
52  
53 the Cueva Pintada zone, the soil structure presents several layers of pyroclastic materials with  
54  
55 some degree of cementation. The thickness of these layers is variable, from 1.5 m thick to  
56  
57 few centimeters in the case of the shallower ones. This structure is named volcanic tuff. The  
58  
59  
60

1  
2  
3 layers have a mainly horizontal stratigraphy, with a slope of less than 5%. Sediments of  
4  
5 variable thickness are the shallowest layer over the tuff. This layer is composed by materials  
6  
7 from the erosion of the upper part of the volcanic structure. In some places, a carbonated  
8  
9 centimeter layer, **originated by organic soil**, covers the surface. Thin layers of about 10 to 40  
10  
11 centimeters **are** intercalated with millimetric layers from the volcanic tuff of Cueva Pintada  
12  
13 complex (Cañaveras et al., 2007). This millimetric layers or sheets are formed by the erosion  
14  
15 of the surrounding layers and, in some of them, appear clays. Sometimes carbonates cement  
16  
17 these layers. This sandwich structure is easily to be appreciated due to the color change and  
18  
19 the differential erosion (Fig 1a.). In fact, each thin layer can be subdivided in thinnest layers  
20  
21 due the differential deposition of the pyroclastic materials during the eruption.  
22  
23  
24  
25  
26  
27  
28  
29

30 The dissolution of tuff silicates into the water **seeping through tuff pores** produces the  
31  
32 carbonate cement. Tuff presents high porosity and, although the rainfall is very low (less than  
33  
34 200 mm per year), the effects of water are clearly visible in the complex of troglodyte caves.  
35  
36 One of the causes was the existence of farms placed on the soil over the **troglodyte caves**  
37  
38 complex, previous to the construction of the museum. Fertilized water irrigates the crop of  
39  
40 the farm. This fact produces a double effect; in one hand, there were more water circulating  
41  
42 and, in the other hand the fertilizer produces, in some places, efflorescences. The chemical  
43  
44 alteration index of Nesbitt and Young (1982, 1989) measured at the troglodyte complex are  
45  
46 between moderated to moderated-high (Hoyos et al., 1998). The variability of the results of  
47  
48 all tests performed at some test-tube extracted from the complex and a near curry is high.  
49  
50  
51  
52

53 As a result, materials of the Cueva Pintada complex present an important weathering with  
54  
55 detachment of little bits of tuff.  
56  
57  
58  
59  
60



### GPR survey

Nine radar lines were carried out with a 900 MHz center frequency antenna, on the roof of Cueva Pintada separated about 0.5 meters (Fig.2) covering the whole of the natural cover. Six of them with a length of about 5.1 meters, Two profiles of 4.9 meters and one of them of about 4.6 meters length. The position of the antenna was assured by an odometer placed in a little trolley down a stick, where the antenna was placed (Fig. 3). The length of the stick was variable in order to assure a distance between the antenna and the roof as little as possible without touching it.

Data was acquired with a 60 ns time window. Data processing consists of the application of a band pass frequency filter with cutoff frequencies of 225 MHz and 1800 MHz.

### Vibration survey

Vibration survey was carried out by means of an accelerometer and a laser Doppler system in order to not damage the cave and its paintings. The accelerometer was a piezoelectric one of B&K 394A10 with flat response from 0.1 to up to 1300 HZ and the Doppler system by a laser Doppler vibrometer PDV100 of Polytec. This is a system based on a Helium-Neon laser with an output power less than 1 mW (class 2) with a frequency range from 0.05 to 22 kHz. The wavelength is 633 nm. This type of LASER is used in heritage conservation without damage for paintings (i.e. Castellini et al, 1996 and 2003). Some applications of Laser Doppler Vibrometer (LDV) use a force engine to produce and input vibration to be compared with the output vibration of each point. In our case, the use of a force engine to produce a vibration of the cave was not possible due to the dimension of the site and its special sensitivity to vibrations. For this reason, an accelerometer was placed on the starting point of

1  
2  
3 the cave roof (covering shelter) in order to have a reference point. An overall peak hold  
4  
5 analysis was used to detect the places where amplification of the vibration were produced.  
6  
7

8 The visual inspection detected cracks, and the layer structure in a centimeter dimension.  
9

10 Therefore, the required accuracy of the results might be on the same order. The long record  
11  
12 time required to perform an overall peak analysis with natural vibration excitation make  
13  
14 impossible to measure in all points with a centimeter accuracy. Using GPR results and the  
15  
16 observed cracks in the natural roof of the cave, we plan the location of 118 measuring points  
17  
18 (Fig. 4) of 360 seconds of record.  
19  
20  
21

22  
23 Surface images were computed by nearest interpolation due to the high variation between  
24  
25 closed points.  
26  
27

28 A concert is played some time in front of the cave. For this reason, an analysis of the  
29  
30 vibration produced by the music equipment used for the concerts was done. Only the point 94  
31  
32 was used to measure possible affections of concert on the cave roof vibration levels. For this  
33  
34 study, the overall peak hold analysis and a Fourier analyses has been computed.  
35  
36  
37  
38  
39  
40

#### 41 **GPR results**

42  
43

44 An average velocity of about 10 cm/ns was estimated using the two-way travel time of the  
45  
46 reflected wave on the upper part of the cave cover. The consequent dielectric constant is  
47  
48 about 11, which corresponds to a high porous volcanic rock (Rust et al., 1999) that is  
49  
50 according with the measured values, around 25%, in some tests of the troglodyte complex  
51  
52 (Hoyos et al., 1998).  
53  
54  
55  
56  
57

58 Radar images shown important anomalies produced by reflections at a depths of about 0.2 m  
59  
60 to 0.8 meters (2 ns to 8 ns) and from 1.5 meters (15 ns) to the top to the roof. These targets

1  
2  
3 seem to present almost horizontal arrangement. Time slices (Fig. 5) indicate the existence of  
4 an important detachment that goes slowly deeper from right to left. Other anomalies could be  
5 associated to cracks. The analysis of the radar images indicates that the zones affected by  
6 inner damage and detachment are more than 50% of the total roof cave.  
7  
8  
9  
10  
11  
12  
13  
14

### 15 **Vibration results**

16  
17  
18 The ratio between overall peak measured in the cave ceiling and in the reference point has  
19 ranged between 0.03 and 91 (Fig. 6). Near half of the ceiling have amplifications over 5 times  
20 and a quarter of it over 25 times. There are 14 measured points with ratios greater than 50.  
21  
22  
23 But also there are 35% under 1 and 5% under 0.1. The surface image computed by nearest  
24 interpolation shows high variation of the amplification in close distances.  
25  
26  
27  
28  
29

30 The rock fall zone was produced near the point 42 with an overall peak ratio of 74, an  
31 important crack and a zone where radar has depicted an inner crack.  
32  
33  
34

35  
36 The maximum vibration on the reference point, at the roof, was only of 0.35 mm/s but in the  
37 ceiling was about 5.6 mm/s. This last value was done with a low reference vibration of 0.062  
38 mm/s so the expected value reached when high reference vibration occurs could be of about  
39  
40  
41  
42  
43  
44  
45  
46  
47  
48  
49  
50  
51  
52  
53  
54

55  
56 Results of average spectra in all the measured points show two main frequencies (around 10  
57 and 15 Hz) that probably correspond to modal modes of the ceil. In general, points with high  
58 amplification show higher amplification of these modal frequencies but also some of them  
59 show other peaks at higher frequencies (Fig. 7).  
60

Results of the concert simulation show overall peak amplification similar to the detected with  
the ambient noise vibration. The vibration level at the reference point produced during the  
concert simulation ( $4,09e-005$  m/s) was a little less than the measured without concert

1  
2  
3 simulation at the same point (7.14E-05). In fact, the overall peak ratio with ambient noise was  
4  
5 5.6 meanwhile the ratio with concert music was 4.4. This fact is produced because the  
6  
7 spectrum of the ambient noise and the concert music are different. The spectrum response of  
8  
9 the point 94 shows a clear amplification at frequency range between 10 to 40 Hz (Fig. 8).  
10  
11 This bandwidth affects only the low register of few instruments as Tuba, Double bass, bass  
12  
13 guitar and piano. The fact that the vibration measured at the reference point during the  
14  
15 concert simulation was so low indicates that the music is irrelevant for the overall study  
16  
17 except for the mentioned frequency bandwidth.  
18  
19  
20  
21  
22  
23  
24

## 25 Conclusions

26  
27  
28 Dielectric constant measured in the roof of the painted cave reveals that the porosity of its  
29  
30 roof is high and similar to the obtained in some tests in the troglodyte complex. This  
31  
32 characteristic of the materials could favor water leaks and, therefore, damage on the paintings  
33  
34 of the troglodyte complex.  
35  
36

37  
38 GPR survey reveals the existence of potential damaged zones covering more than the 50% of  
39  
40 the surface of the roof. In addition, the images highlight the existence of important cracks.  
41  
42 The analysis of the results denotes the position and the practically horizontal layout of the  
43  
44 most important cracks. Radar data was used in the planning of the subsequent vibration  
45  
46 survey. Zones with more anomalies associated to inner cracks were densely studied with  
47  
48 passive seismic, using a higher number of vibration measurement points.  
49  
50

51  
52 The surface image computed by nearest interpolation shows high variation of the  
53  
54 amplification that is produced by the layer structure of the cave roof. There are some sheets  
55  
56 that have high amplifications of ambient noise vibrations reaching 91 times. The ratio  
57  
58 between overall peak measured in the cave ceiling and in the reference point has ranged  
59  
60

1  
2  
3 between 0.03 and 91, near half of the ceiling have amplifications over 5 times and a quarter  
4 of it over 25 times. There are 14 measured points with ratios greater than 50. But also there  
5  
6 are 35% under 1 and 5% under 0.1. The surface image computed by nearest interpolation  
7  
8 shows high variation of the amplification in close distances.  
9  
10

11  
12  
13 The rock fall zone was produced near the point 42 with an overall peak ratio of 74, an  
14  
15 important crack and a zone were radar has depicted an inner crack.  
16  
17

18  
19 The maximum vibration on the reference point, at the roof, was only of 0.35 mm/s but in the  
20  
21 ceiling was about 5.6 mm/s. This last value was done with a low reference vibration of 0.062  
22  
23 mm/s so; the expected value reached when high reference vibration occurs could be of about  
24  
25 31 mm/s.  
26  
27

28  
29 These high amplifications measured in some zones of the cave roof recommend decreasing  
30  
31 the **ambient** noise vibration as much as possible.  
32  
33

34  
35 The music concerts not affect significantly the cave except for low record of some  
36  
37 instruments as tuba, double bass, bass guitar and piano in the frequency range between 10 to  
38  
39 40 Hz.  
40  
41  
42  
43

#### 44 **Acknowledgment**

45  
46  
47

48  
49 This research was partially funded by the Ministry of Economy and Competitiveness  
50  
51 (MINECO) of the Spanish Government and by the European Regional Development Fund  
52  
53 (FEDER) of the European Union (UE) through the project referenced as CGL2015-65913-P  
54  
55 (MINECO/ FEDER, UE).  
56  
57  
58  
59  
60

## References

- Beres, M., Luetscher, M., Olivier, R., 2001. Integration of ground-penetrating radar and microgravimetric methods to map shallow caves. *Journal of Applied Geophysics* 46(4), 249-262.
- Borri, A., Grazini, A., 2006. Diagnostic analysis of the lesions and stability of Michelangelo's David. *Journal of cultural heritage* 7, 273-285.
- Cañaveras Jimenez, J.C., Sanz Rubio, E, Sanchez Moral, S., Hoyos Gómez, M., 2007. Las alteraciones de los materiales volcánicos encajantes del complejo troglodita de la Cueva Pintaada: ecología, petrología y geoquímica. *Cuadernos de Patrimonio Histórico* 7. 59-81.
- Caselles, O., Clapes, J., Elyamani, A., Lana, J., Seguí, C., Martín, A., Roca, P., 2018. Damage detection using principal component analysis applied to temporal variation of natural frequencies. In: *Proceedings of the 16<sup>th</sup> European Conference on Earthquake Engineering*. Thessalonica, Greece.
- Castellini, P., Paone, N., Tomasini, E.P., 1996. The laser doppler vibrometer as an instrument for nonintrusive diagnostic of works of art: Application to fresco paintings. *Optics and lasers in engineering* 25, 227-246.
- Castellini, P., Esposito, E., Marchetti, B., Paone, N., Tomasini, E.P., 2003. New applications of scanning laser doppler vibrometer (SLDV) to non-destructive diagnostic of artworks: mosaics, ceramics, inlaid wood and easel painting. *Journal of cultural heritage* 4, 321-329.
- Cataldo, R., De Donno, A., De Nunzio, G., Leucci, G., Nuzzo, L., Siviero, S., 2005. Integrated methods for analysis of deterioration of cultural heritage: the Crypt of "Cattedrale di Otranto". *Journal of cultural heritage* 6(1), 29-38.

- 1  
2  
3 Čeru, T., Šegina, E., Knez, M., Benac, Č., Gosar, A., 2018. Detecting and characterizing  
4 unroofed caves by ground penetrating radar. *Geomorphology* 303, 524-539.  
5  
6  
7  
8 Ferrara, C., Barone, P. M., 2015. Detecting moisture damage in archaeology and cultural  
9 heritage sites using the GPR technique: a brief introduction. *International Journal of*  
10 *Archaeology* 3(1-1), 57-61.  
11  
12  
13  
14  
15  
16 Fukuda, Y., Feng, M.Q., Shiunozuka, M., 2010. Cost-effective vision-based system for  
17 monitoring dynamic response of civil engineering structures. *Structural Control and Health*  
18 *Monitoring* 17, 918–936.  
19  
20  
21  
22  
23  
24 González-Drigo, R., Pérez-Gracia, V., Di Capua, D., Pujades, L. G., 2008. GPR survey  
25 applied to Modernista buildings in Barcelona: The cultural heritage of the College of  
26 Industrial Engineering. *Journal of Cultural Heritage* 9(2), 196-202.  
27  
28  
29  
30  
31 Gracia, V. P., Canas, J. A., Pujades, L. G., Clapés, J., Caselles, O., Garcia, F., Osorio, R.,  
32 2000. GPR survey to confirm the location of ancient structures under the Valencian Cathedral  
33 (Spain). *Journal of Applied Geophysics* 43(2-4), 167-174.  
34  
35  
36  
37  
38 Hoyos Gómez, M. , Sanchez Moral, S., Sanz Rubio, E., Cañaveras Jimenez, J.C., 1998.  
39 Informe sobre la alteración de los materiales volcánicos encajantes del complejo troglodita de  
40 Galdar (Gran Canaria). CSIC, Madrid.  
41  
42  
43  
44  
45  
46 Nesbitt, H.W., Young, G.M., 1982. Early proterozoic climates and plate motion inferred from  
47 major element chemistry of lutites. *Nature*, 299, 715-717.  
48  
49  
50  
51 Nesbitt, H.W., Young, G.M., 1989. Formation and diagnosis of weathering profiles. *Journal*  
52 *of Geology* 97, 129-147.  
53  
54  
55  
56  
57 Nunziata, C., Mele, R., Natale, M., 1999. Shear wave velocities and primary influencing  
58 factors of Campi Flegrei–Neapolitan deposits. *Engineering Geology* 54, 299–312  
59  
60

1  
2  
3 Nuzzo, L., Leucci, G., Negri, S., Carrozzo, M. T., Quarta, T., 2002. Application of 3D  
4 visualization techniques in the analysis of GPR data for archaeology. *Annals of Geophysics*  
5  
6 45(2).  
7  
8

9  
10 Pérez-Gracia, V., Caselles, J. O., Clapes, J., Osorio, R., Martínez, G., Canas, J. A., 2009a.  
11 Integrated near-surface geophysical survey of the Cathedral of Mallorca. *Journal of*  
12  
13 *Archaeological Science* 36(7), 1289-1299.  
14  
15

16  
17 Pérez-Gracia, V., Caselles, O., Clapés, J., Osorio, R., Canas, J. A., Pujades, L. G., 2009b.  
18  
19 Radar exploration applied to historical buildings: a case study of the Marques de Llió palace,  
20  
21 in Barcelona (Spain). *Engineering Failure Analysis* 16(4), 1039-1050.  
22  
23

24  
25 Pérez-Gracia, V., González-Drigo, R., Sala, R., 2012. Ground-penetrating radar resolution in  
26  
27 cultural heritage applications. *Near Surface Geophysics* 10(°1), 77-87.  
28  
29

30  
31 Pérez-Gracia, V., Caselles, J. O., Clapés, J., Martínez, G., Osorio, R., 2013. Non-destructive  
32  
33 analysis in cultural heritage buildings: Evaluating the Mallorca cathedral supporting  
34  
35 structures. *NDT & E International* 59, 40-47.  
36  
37

38  
39 Porsani, J. L., de Matos Jangelme, G., Kipnis, R., 2010. GPR survey at Lapa do Santo  
40  
41 archaeological site, Lagoa Santa karstic region, Minas Gerais state, Brazil. *Journal of*  
42  
43 *archaeological science* 37(6), 1141-1148.  
44  
45

46  
47 Quagliarini, E., Esposito, E., del Conte, A., 2013. The combined use of IRT and LDV for the  
48  
49 investigation of historical thin vaults. *Journal of cultural heritage* 14, 122-128.  
50

51 Doi:10.1016/j.culher.2012.01.004  
52

53  
54 Ranalli, D., Scozzafava, M., Tallini, M., 2004. Ground penetrating radar investigations for  
55  
56 the restoration of historic buildings: the case study of the Collemaggio Basilica (L'Aquila,  
57  
58 Italy). *Journal of cultural heritage* 5(1), 91-99.  
59  
60



1  
2  
3 Rust, A.C., Rusell, J.K., Kgnight, R.J., 1999. Dielectric constant as a predictor of porosity in  
4 dry volcanic rocks. *Journal of volcanology and geothermal research* 91, 76-96.  
5  
6

7  
8 Santos-Assunção, S., Perez-Gracia, V., Caselles, O., Clapes, J., Salinas, V., 2014.  
9

10 Assessment of complex masonry structures with GPR compared to other non-destructive  
11 testing studies. *Remote Sensing* 6(9), 8220-8237.  
12  
13

14  
15 Santos-Assunção, S., Dimitriadis, K., Konstantakis, Y., Perez-Gracia, V., Anagnostopoulou,  
16 E., Gonzalez-Drigo, R., 2016. Ground-penetrating radar evaluation of the ancient Mycenaean  
17 monument Tholos Acharnon tomb. *Near Surface Geophysics* 14(2), 197-205.  
18  
19

20  
21 Siringoringo, D.M., Fujino, Y., 2009. Noncontact operational modal analysis of structural  
22 members by laser doppler vibrometer. *Computer-Aided Civil and Infrastructure Engineering*  
23 24, 249–265.  
24  
25

26  
27 Soler Javaloyes, V., Torres González, P.A., Moure García, A.P., 2007. Registro de  
28 vibraciones y análisis del fondo sísmico en el entorno de la Cueva Pintada de Gáldar.  
29 *Cuadernos de Patrimonio Histórico* 7, 125-132.  
30  
31

32  
33 Solla, M., Lorenzo, H., Rial, F. I., Novo, A., 2011. GPR evaluation of the Roman masonry  
34 arch bridge of Lugo (Spain). *NDT & E International* 44(1), 8-12.  
35  
36

37  
38 Sternberg, B. K., McGill, J. W., 1995. Archaeology studies in southern Arizona using ground  
39 penetrating radar. *Journal of Applied Geophysics* 33(1-3), 209-225.  
40  
41

42  
43 Swanson, P., 2002. Feasibility of using laser-based vibration measurements to detect roof fall  
44 hazard in underground mines. In: *Proceedings of the 5<sup>th</sup> Int. Conf. on Vibration  
45 Measurements by Laser Techniques*. Ancoma, Italy  
46  
47  
48  
49  
50  
51  
52  
53  
54  
55  
56  
57  
58  
59  
60

- 1  
2  
3 Waldron, K., Ghoshal, A., Schulz, M. J., Sundaresan, M. J., Ferguson, F., Pai, P. F., Chung, J.  
4  
5 H., 2002. Damage detection using finite element and laser operational deflection shapes,  
6  
7 *Finite Elements in Analysis and Design* 38(3), 193–226.  
8  
9  
10 Whiting, B. M., McFarland, D. P., Hackenberger, S., 2001. Three-dimensional GPR study of  
11  
12 a prehistoric site in Barbados, West Indies. *Journal of Applied Geophysics* 47(3-4), 217-226.  
13  
14  
15 Zarandieta, L., Sosa, J.M., Feduchi J., 2007. El proyecto arquitectónico del museo y parque  
16  
17 arqueológico de la Cueva Pintada: Una intervención para la conservación Cuadernos de  
18  
19 Patrimonio Histórico 7. 219-251  
20  
21  
22  
23 Zhao, W., Forte, E., Pipan, M., Tian, G., 2013. Ground penetrating radar (GPR) attribute  
24  
25 analysis for archaeological prospection. *Journal of Applied Geophysics* 97, 107-117.  
26  
27  
28 Zhao, W., Forte, E., Levi, S. T., Pipan, M., Tian, G., 2015. Improved high-resolution GPR  
29  
30 imaging and characterization of prehistoric archaeological features by means of attribute  
31  
32 analysis. *Journal of Archaeological Science* 54, 77-85.  
33  
34  
35  
36  
37  
38  
39  
40  
41  
42  
43  
44  
45  
46  
47  
48  
49  
50  
51  
52  
53  
54  
55  
56  
57  
58  
59  
60

## FIGURE CAPTION

Figure 1. Cueva Pintada. a) The **sandwiched** layer structure is appreciated in the walls and in the roof. b) Outside view of the museum complex designed as a typical Canarian greenhouse remembering the old use of the emplacement (Zarandieta et al., 2007). c) Maps of the location.

Figure 2. Map of the painted cave with the location of the radargram (straight lines marked with R1 to R9), **rock fall** produced at begin of 2016 (cercle), the natural cave (black line) and reinforced concrete cover (red line).

Figure 3. Photography of the trolley developed to carry out the GPR survey.

Figure 4. Location of the planned measuring points. In **red** the zones where GPR has detected inner cracks.

Figure 5. 3D GPR images.

Figure 6. Overall **peak** ratio of the cave ceiling. In grey main surface cracks. Black circle marks the **rock fall** zone of 2016.

1  
2  
3 Figure 7. Autospectra of LASER vibrometer in different places.  
4  
5

6 Figure 8. Autospectra of fixed accelerometer (continuous line) and LASER vibrometer  
7 (dashed line) at reference point 94 during simulation concert (dark lines) and without  
8 simulation concert (gray lines).  
9  
10  
11  
12  
13  
14  
15  
16  
17  
18  
19  
20  
21  
22  
23  
24  
25  
26  
27  
28  
29  
30  
31  
32  
33  
34  
35  
36  
37  
38  
39  
40  
41  
42  
43  
44  
45  
46  
47  
48  
49  
50  
51  
52  
53  
54  
55  
56  
57  
58  
59  
60

For Peer Review Only



Figure 1. Cueva Pintada. a) The sandwiched layer structure is appreciated in the walls and in the roof. b) Outside view of the museum complex designed as a typical Canarian greenhouse remembering the old use of the emplacement (Zarandieta et al., 2007). c) Maps of the location.

280x49mm (300 x 300 DPI)

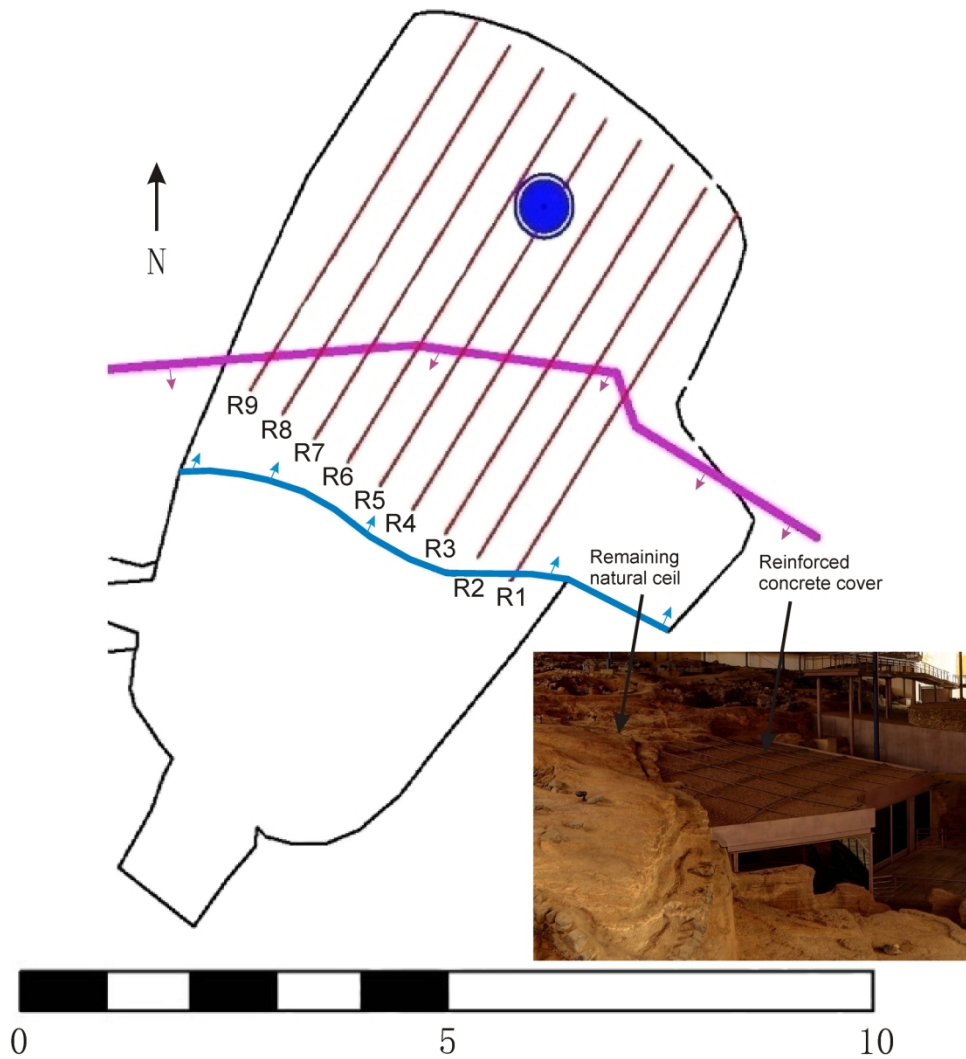
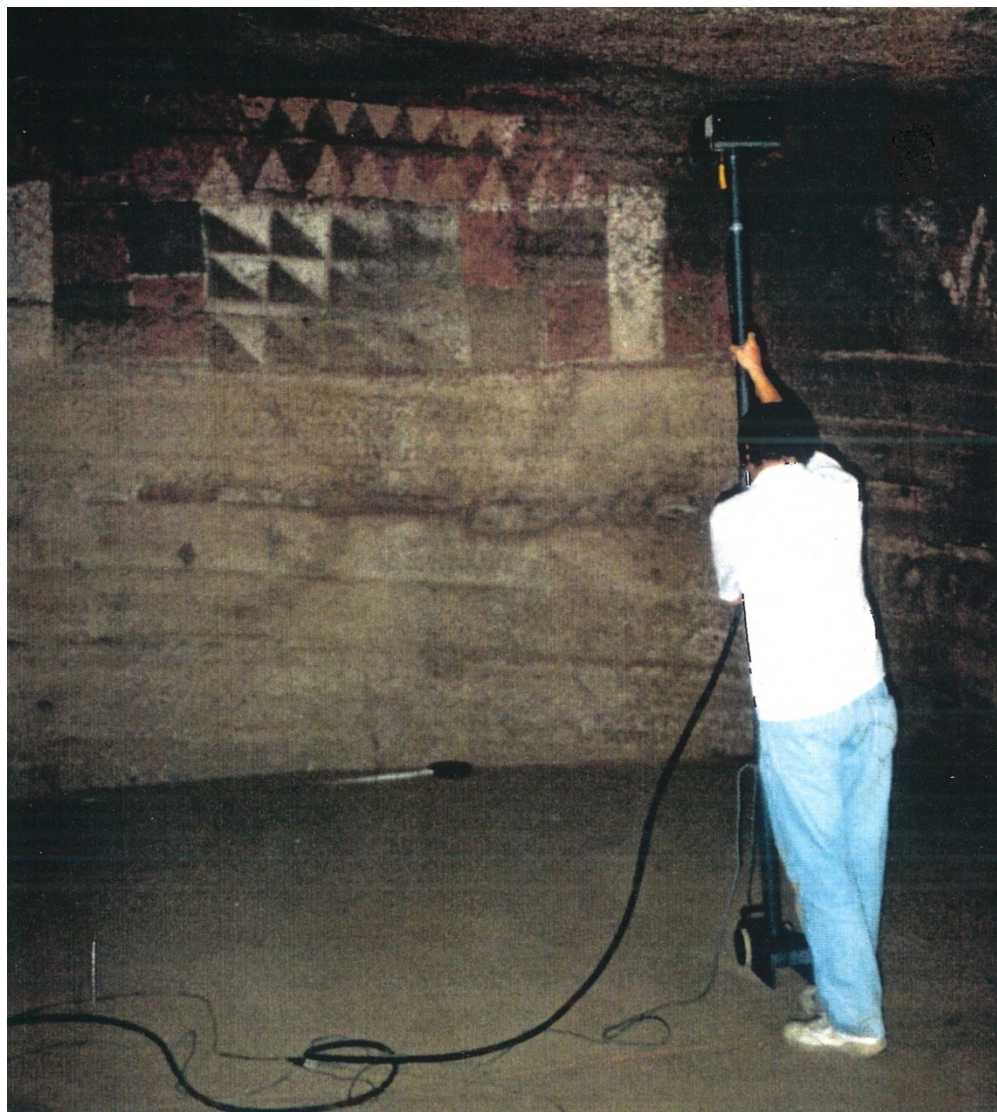


Figure 2. Map of the painted cave with the location of the radargram (straight lines marked with R1 to R9), rock fall produced at begin of 2016 (cercle), the natural cave (black line) and reinforced concrete cover (red line).

224x257mm (300 x 300 DPI)



42 Figure 3. Photography of the trolley developed to carry out the GPR survey.

43  
44 602x668mm (96 x 96 DPI)

1  
2  
3  
4  
5  
6  
7  
8  
9  
10  
11  
12  
13  
14  
15  
16  
17  
18  
19  
20  
21  
22  
23  
24  
25  
26  
27  
28  
29  
30  
31  
32  
33  
34  
35  
36  
37  
38  
39  
40  
41  
42  
43  
44  
45  
46  
47  
48  
49  
50  
51  
52  
53  
54  
55  
56  
57  
58  
59  
60

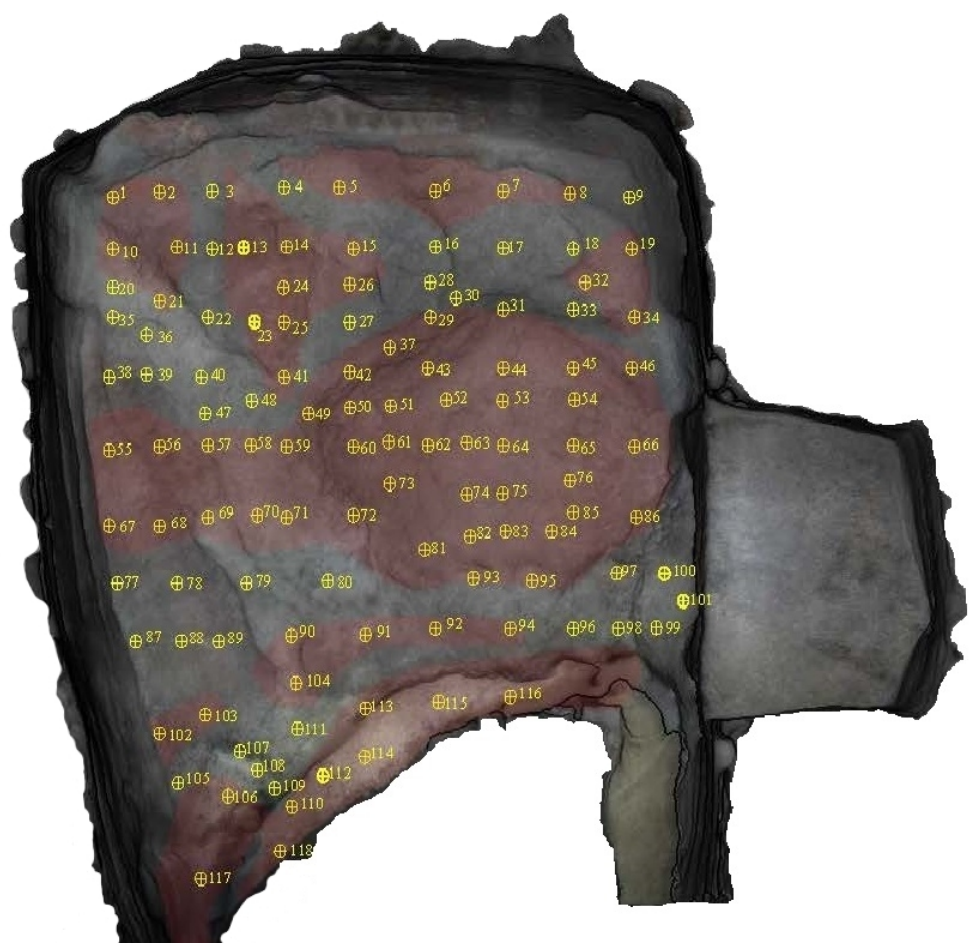


Figure 4. Location of the planned measuring points. In red the zones where GPR has detected inner cracks.

243x231mm (87 x 87 DPI)



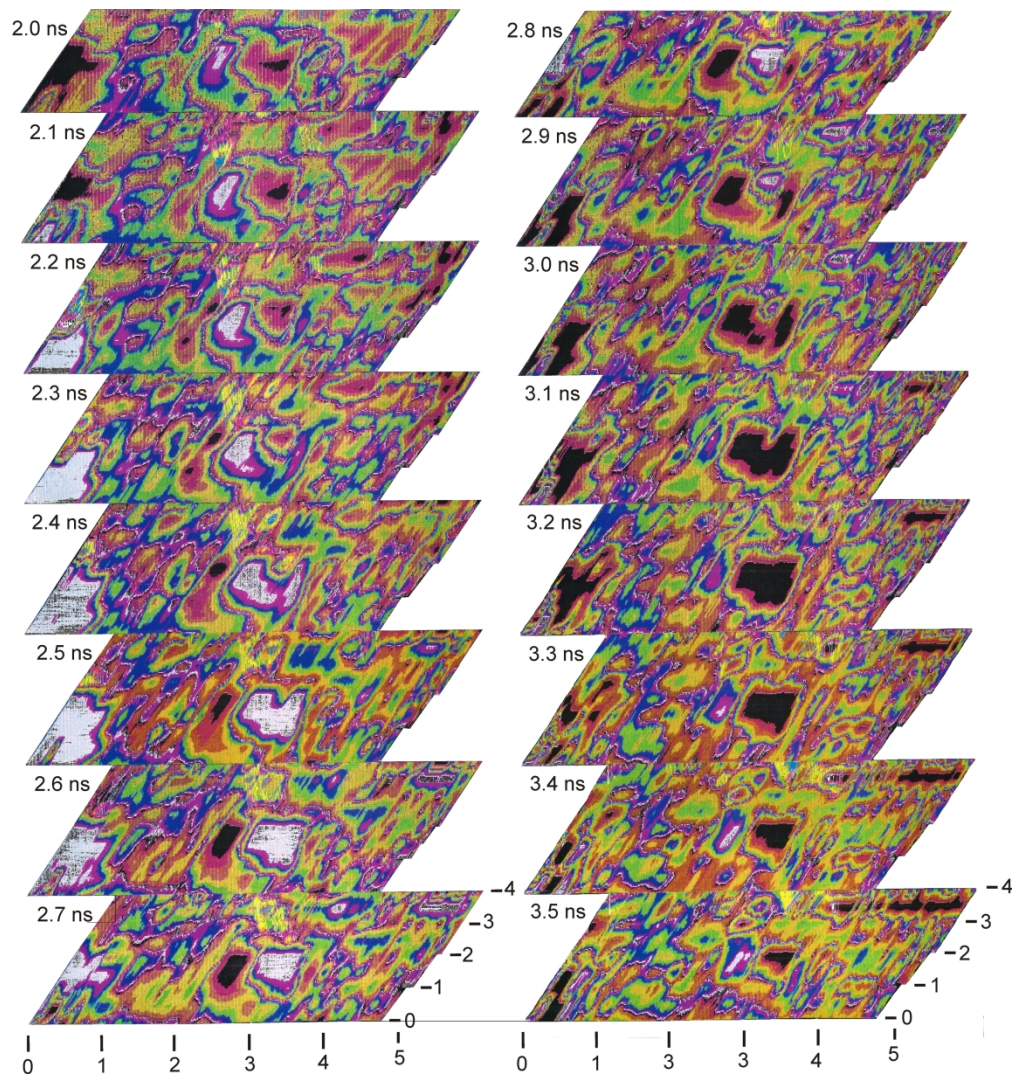


Figure 5. 3D GPR images.

275x293mm (300 x 300 DPI)

1  
2  
3  
4  
5  
6  
7  
8  
9  
10  
11  
12  
13  
14  
15  
16  
17  
18  
19  
20  
21  
22  
23  
24  
25  
26  
27  
28  
29  
30  
31  
32  
33  
34  
35  
36  
37  
38  
39  
40  
41  
42  
43  
44  
45  
46  
47  
48  
49  
50  
51  
52  
53  
54  
55  
56  
57  
58  
59  
60

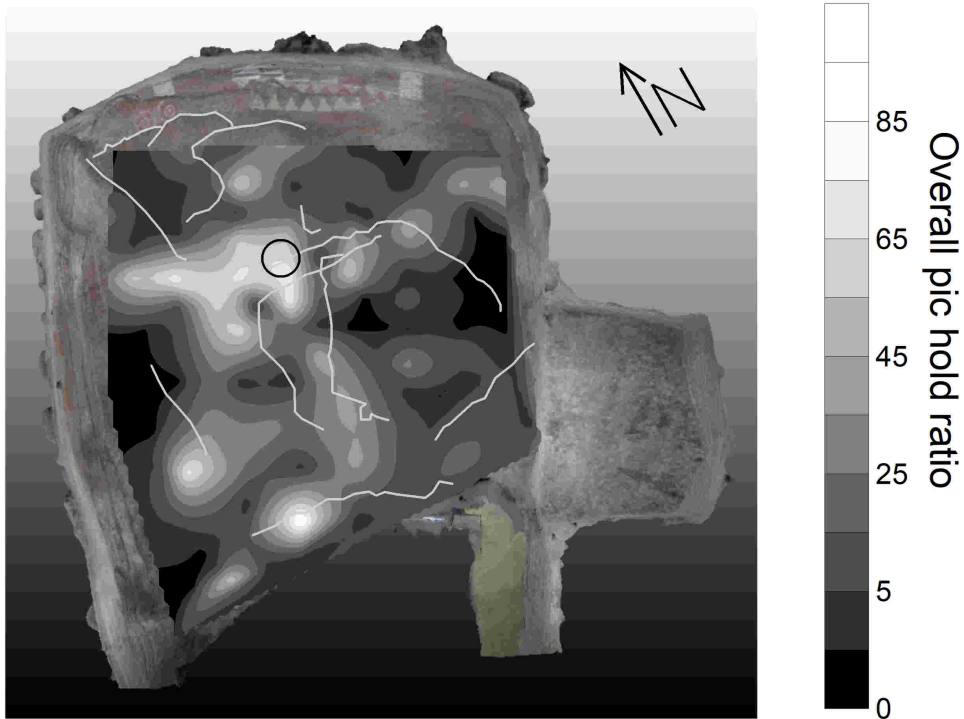


Figure 6. Overall pic ratio of the cave ceiling. In grey main surface cracks. Black circle marks the landslide zone of 2016.

694x574mm (93 x 93 DPI)

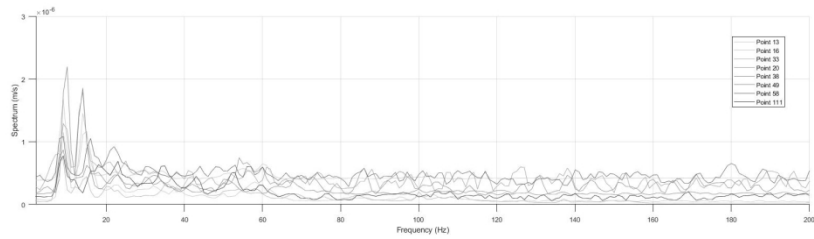


Figure 7. Autospectra of LASER vibrometer in different places.

677x255mm (72 x 72 DPI)

1  
2  
3  
4  
5  
6  
7  
8  
9  
10  
11  
12  
13  
14  
15  
16  
17  
18  
19  
20  
21  
22  
23  
24  
25  
26  
27  
28  
29  
30  
31  
32  
33  
34  
35  
36  
37  
38  
39  
40  
41  
42  
43  
44  
45  
46  
47  
48  
49  
50  
51  
52  
53  
54  
55  
56  
57  
58  
59  
60

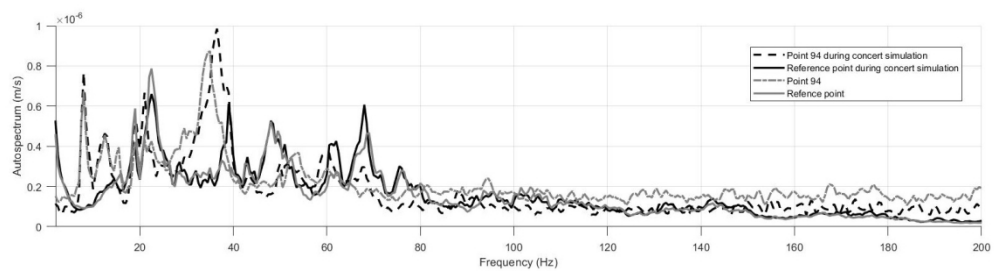


Figure 8. Autospectra of fixed accelerometer (continuous line) and LASER vibrometer (dashed line) at reference point 94 during simulation concert (dark lines) and without simulation concert (gray lines).

340x91mm (120 x 120 DPI)